11th Australasian Fluid Mechanics Conference
University of Tasmania, Hobart, Australia
14-18 December 1992

A STUDY OF THE KINEMATICS AND TOPOLOGY OF UNSTEADY CONFINED SWIRLING FLOWS

C.J. BULBECK[1], J.M. LOPEZ[2] and J. SORIA[3]

[1]DSTO - Aeronautical Research Laboratory, Fishermens Bend, VIC 3207, AUSTRALIA

[2]Pennsylvania State University, University Park PA 16802, USA

[3]CSIRO Div of Building Construction & Engineering, PO Box 56, Highett, VIC 3190, AUSTRALIA

ABSTRACT

Complex fluid motions may result when the fluid inside a completely filled cylinder is driven by the constant rotation of the bottom endwall. At low rotation rates, the flow is steady and axisymmetric vortex breakdown is possible. At higher rotation rates, a Hopf bifurcation takes place resulting in a periodic unsteady flow. The kinematics of the calculated flow are investigated by classifying the local topology as determined from the invariants of the velocity gradient tensor. The principal strain directions are determined and the alignment of the vorticity vector with these directions is investigated, particularly in the vortex breakdown region. The topological features identified in this idealised flow are expected to be universal to all processes involving vortex breakdown.

INTRODUCTION

With the advent of full numerical calculations of the Navier-Stokes equations, it has become possible to study the details of complicated flows. In contrast to previous analyses of unsteady flows where only mean quantities and simple correlations could be considered, it is now possible to study both spatial and temporal distributions of any flow quantity. Even quantities which are difficult to measure in a physical experiment, such as the vorticity, are now available. New methods of investigating the large data bases produced by such calculations have had to be developed. A good starting point for understanding complex unsteady flows is to study the kinematics and the invariant character of the topology of such flows.

GLOBAL AND LOCAL CLASSIFICATIONS OF FLOWFIELD TOPOLOGIES

Complex flow fields can be interpreted by classifying their topology. This can either be done *globally* or *locally*. In the global approach, developed by Perry and Fairlie (1974) and extended by Chong, Perry and Cantwell (1990), the critical points of the flowfield are identified. The critical points in a flowfield are those points where all three velocity components are zero relative to a global observer. A local Taylor series expansion of the velocity field with respect to space coordinates is made at each of these critical points, and the invariants of the resulting 3×3 Jacobian matrix, the velocity gradient tensor A_{ij}, are used to completely classify the topology of this critical point.

In the local approach the coordinate system follows the fluid particle without rotation. That is, each point in the flowfield is considered to be a critical point, since the velocity of each point is zero relative to a local observer. The topology of each point in the flow is then classified as in the global approach by considering the local velocity gradient tensor at each point in the flow. Due to the Galilean invariant nature of the velocity gradient tensor, and hence any property based on this tensor, the local topological classification of each fluid flow point is independent of the observer. This local classification of the flowfield was first used by Chen *et al.* (1990) and is the approach used in this study.

The velocity gradient tensor can be decomposed into its symmetric and antisymmetric parts, i.e.

$$A_{ij} = \frac{\partial u_j}{\partial x_i} = S_{ij} + R_{ij},$$

where

$$S_{ij} = \left(\frac{\partial u_i}{\partial x_j} + \frac{\partial u_j}{\partial x_i}\right)/2,$$

is the rate-of-strain tensor and

$$R_{ij} = \left(\frac{\partial u_i}{\partial x_j} - \frac{\partial u_j}{\partial x_i}\right)/2,$$

is the rotation tensor. A_{ij}, S_{ij} and R_{ij} are all tensors of second order.

For a second order tensor, $\mathbf{A}$, if λ_1, λ_2 and λ_3 are the eigenvalues and e_1, e_2 and e_3 are the eigenvectors, then

$$(\mathbf{A} - \lambda \mathbf{I})e = \mathbf{0},$$

and the corresponding characteristic equation

$$\det[\mathbf{A} - \lambda \mathbf{I}] = 0,$$

may be written as

$$\lambda^3 + P\lambda^2 + Q\lambda + R = 0.$$

The invariants P, Q and R are

$$P = -S_{ii},$$

$$Q = (P^2 - S_{ij}S_{ji} - R_{ij}R_{ji})/2,$$

$$R = (-P^3 + 3PQ - S_{ij}S_{jk}S_{ki} - 3R_{ij}R_{jk}S_{ki})/3.$$

For an incompressible flow, as is being considered here, $P = 0$, and the topology of the flow is completely classified by Q and R.

The characteristic equation, $\lambda^3 + Q\lambda + R = 0$, can have (*i*) all real distinct roots, (*ii*) all real roots with at least two equal, or (*iii*) one real root and a pair of complex conjugate roots. The curve $27R^2 + 4Q^3 = 0$, separates the regions of real and complex roots. Chong, Perry and Cantwell (1990) defined regions where the velocity gradient tensor has complex eigenvalues as vortex cores, i.e. regions where $Q > -3(R/2)^{2/3}$ are vortical in nature. The eigenvalues of the velocity gradient tensor determine the local kinematics of the flow, and these are determined by the invariants Q and R. If $Q > -3(R/2)^{2/3}$, then a pair of complex conjugate eigenvalues result and the trajectories will spiral locally. Whether the spirals are stable or unstable is determined by the sign of the real eigenvalue, which in turn is determined by the sign of R. If $R > 0$, then the spiral is unstable and to conserve mass, the local topology is of the unstable focus/contracting type. For $R < 0$, it is of the stable focus/stretching type. For the degenerate case of $R = 0$, the trajectory is a closed loop, rather than a spiral. For $Q < -3(R/2)^{2/3}$, the local flow is strain dominated and for $R < 0$ the topology is of the stable node/saddle/saddle type and for $R > 0$ it is of the unstable node/saddle/saddle type.

The eigenvectors of the rate-of-strain tensor, S_{ij}, are known as the principal strain rate directions. The corresponding eigenvalues, the principal strain rates, are real, since S_{ij} is symmetric, and if they are distinct, then the principal strain rate directions are orthogonal. If two of the eigenvalues are equal, then the principal strain rate direction corresponding to the remaining eigenvalue is uniquely determined, except for the sense of its direction. The other two can be any vector in the plane normal to the first principal strain rate direction, and in particular they can be any two orthogonal vectors in the plane. If all three eigenvalues are equal, then any vector can be taken as a principal strain rate direction, and in particular they may be any three orthogonal vectors.

SWIRLING FLOW IN AN ENCLOSED CYLINDER

Consider a circular cylinder, of radius R and height H, completely filled with an incompressible fluid of constant kinematic viscosity, ν. At time $t = 0$, when the fluid and the cylinder are at rest, the bottom endwall is impulsively set to rotate at a constant angular speed Ω. This flow is completely specified by two non-dimensional parameters. These are the aspect ratio of the cylinder H/R, and the rotational Reynolds number $Re = \Omega R^2/\nu$.

When the bottom endwall is impulsively started, a thin Ekman boundary layer (with constant thickness of order $Re^{-1/2}$) is formed which centrifuges fluid outwards while drawing fluid from above to maintain conservation of mass. The expelled fluid then spirals up the sidewall, forming another boundary layer from which a portion of the angular momentum and total head acquired in the Ekman layer is transferred to the interior flow through the action of viscous stresses. This sidewall boundary layer is deflected at the upper endwall and an upper endwall boundary layer is formed. The endwall boundary layer separates at $r = 0$, forming a central vortex which returns fluid back towards the Ekman boundary layer. In a region of $Re - H/R$ parameter space, this central vortex undergoes vortex breakdown, as detailed in Lopez (1990) and Brown and Lopez (1990). The flow remains axisymmetric up to fairly high Reynolds numbers as demonstrated by the experiments of Escudier (1984).

The details of the equations and boundary conditions used to calculate the flow field are given in Lopez (1990). Here, however, instead of using the axisymmetric form of the Navier-Stokes equations cast in the stream function vorticity formulation and integrated using a time-accurate finite-difference technique, a time-accurate pseudo-spectral formulation for the axisymmetric primitive variables form of the Navier-Stokes equations using the tau method to impose boundary conditions was used, following the method detailed by Tuckerman (1989). One of the attractions of using a spectral representation of the flow is the availability of high order spatial derivatives to accurately calculate the velocity gradient tensor and other related tensors. Spectral differentiation, using well known recursive formulae, is much more accurate than using finite differences.

RESULTS AND DISCUSSION

The plot of the streamfunction in figure 1(*a*) clearly shows where the vortex breakdown bubbles are formed along the axis of symmetry for the steady case of $Re = 2126$ and $H/R = 2.5$. The corresponding spatial distributions of the three components of vorticity are shown in figures 1(*b*) - (*d*). In the vicinity of the axis of symmetry the radial component of vorticity, ω_r, is approximately zero except for a region just upstream of the upper bubble where it is negative. Along the rotating and stationary endwalls, ω_r is found to be positive. The most striking feature of the vorticity field is the distribution of the vertical component of vorticity, ω_z. In the core region, including the rotating endwall, ω_z is positive, while in the side wall boundary layer it is negative. There is a region separating these areas and including the stationary endwall in which ω_z is almost zero. This naturally divides the flow into an inner and an outer region, where in the inner region the angular momentum of the flow increases with radial distance from the axis, while in the outer region the angular momentum decreases with radial distance. (Note that $\omega_z = 1/r\partial(rv)/\partial r$). This feature of the ω_z distribution is also observed in higher Reynolds number cases for which the flow is unsteady. The vorticity field shows that the flow is laminar with no small scale flow structures , other than the thin Ekman layer on the rotating endwall.

As far as the flow classification using the invariants of the velocity gradient tensor is concerned, this axisymmetric flow is interesting, since it exhibits all the possible three-dimensional incompressible flow topologies. This characteristic can be attributed solely to the swirl in this flow. The topology map in figure 2(*a*) shows that most of this flow is either stable focus/stretching or unstable focus/contracting and hence vortical in nature. Comparing figures 1(*d*) and 2(*a*), the line which separates the vortical region from the strain dominated region coincides reasonably well with the line $\omega_z = 0$. In addition, most of the focal regions are stretching foci, hence, the strain field is such that the vorticity aligns with the positive principal strain rates. However, in the region of the vortex breakdown bubble, there is a switch from a stable focus/stretching topology to an unstable focus /contracting topology. It is interesting that this switch from stable to unstable focus type topology, which occurs when the third invariant of the velocity gradient tensor, R, vanishes, corresponds precisely with $\partial\psi/\partial z = 0$. This may be seen

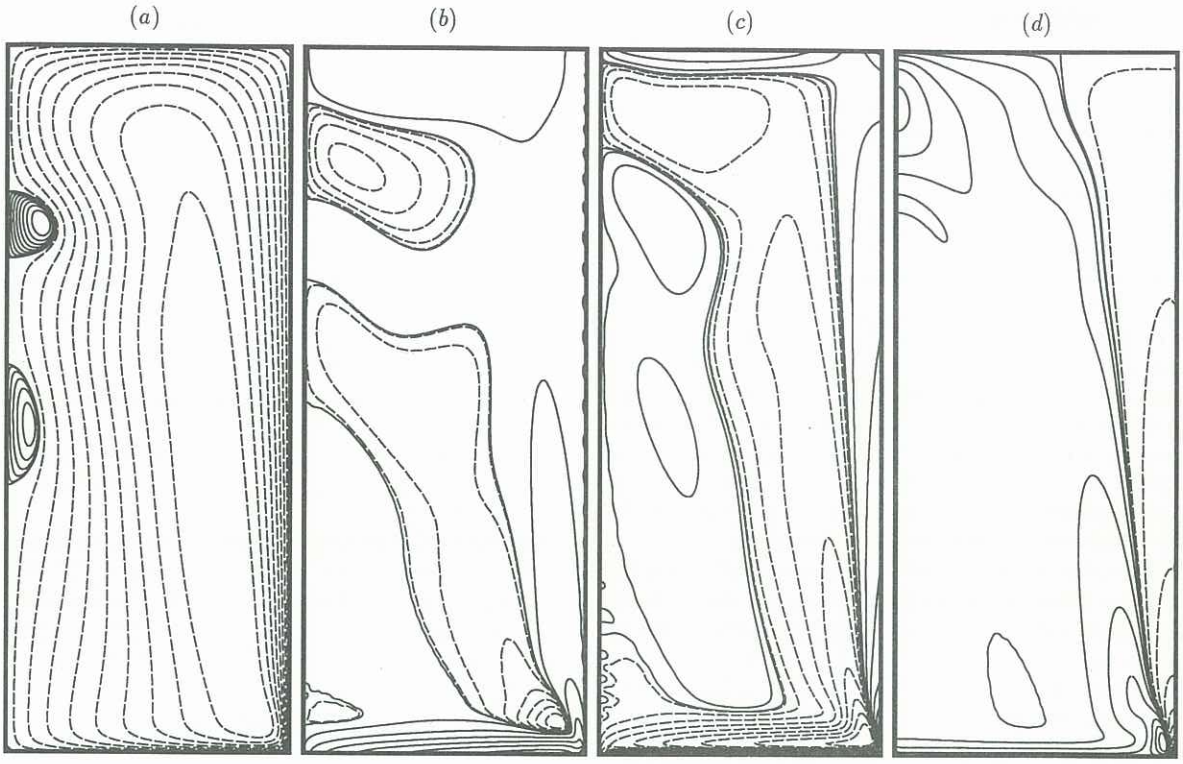

Figure 1: Contours of (a) streamfunction, (b) radial component of vorticity, ω_r (c) azimuthal component of vorticity, ω_θ and (d) vertical component of vorticity, ω_z. The contour levels are non-uniformly spaced, with 10 positive and 10 negative levels determined by c-level(i)=Max($variable$) $\times(i/10)^3$ and c-level(i)=Min($variable$) $\times(i/10)^3$ respectively.

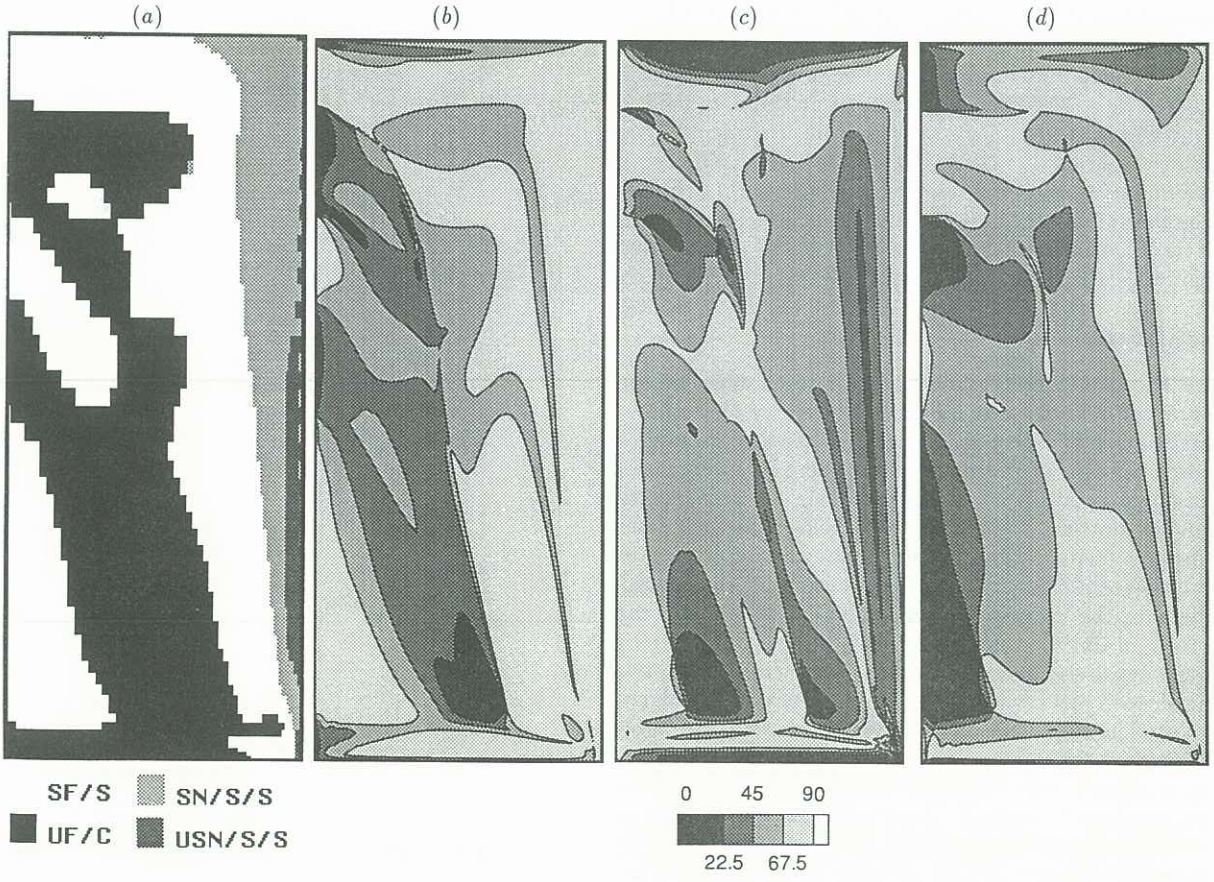

Figure 2: (a) Topology map. Contours of alignment between vorticity and the strain direction corresponding to (b) the largest negative eigenvalue (c) the intermediate eigenvalue (c) the largest positive eigenvalue

in figures 1(*a*) and 2(*a*).

In the unstable focus/contracting topology, the vorticity aligns itself predominantly with the compressive principal strain rates. Figures 2(*b*) and (*d*) which show the alignment between the vorticity vector and the smallest (compressive) and the largest (stretching) principal strain rates bear this feature out quite clearly. In the vicinity of the axis of symmetry, one observes that upstream and in the upper part of both bubbles the vorticity is aligned with the smallest principal strain rate direction, and hence the largest and intermediate principal strain rate directions are perpendicular to the vorticity vector. It can actually be shown that on the axis of symmetry, two principal strains are always equal, hence, the particular alignment just described corresponds to axisymmetric compression. Downstream of this region, i.e. in the lower part of the bubbles, the vorticity aligns with the largest principal strain direction. In these regions and along the axis the flow corresponds to axisymmetric stretching.

In the Ekman layer on the rotating endwall and in the boundary layer on the stationary endwall the vorticity aligns itself with the intermediate principal strain rate direction, whereas in the sidewall boundary layer, the vorticity is not aligned with any of the principal directions. Just outside the sidewall boundary layer, where $\omega_\theta = 0$, the vorticity is aligned with the intermediate principal strain direction. In the region identified in figure 1(*d*), where ω_z is nearly zero and which divides the flow into inner and outer regions, one observes that the alignment between the strain field and the vorticity is such that the vorticity vector is perpendicular to the smallest principal strain rate and is at approximately 45 degrees to the intermediate and the largest principal strain rate directions.

The same observations were made for the periodic case of $Re = 2765$. The unsteadiness in the flow field is mirrored in the topology map and the alignments. The switch from stable to unstable focal topology still occurs where $\partial\psi/\partial z = 0$. There are no changes in the local topology throughout the period of the oscillation, just as there is no change in the topology of the Poincaré map for this periodic case (Lopez and Perry, 1992).

SUMMARY

The axisymmetric vortex breakdown flow in the enclosed cylinder can be characterised by the following kinematic features. Along the axis of symmetry and upstream of the breakdown, there is a change in topology from stable focus/stretching to unstable focus/contracting. Similarly, the topology changes from unstable focus/contracting to stable focus/stretching in the downstream part of the breakdown region. Along the axis, the vorticity vector is aligned either with the principal direction associated with the most positive or most negative eigenvalue of the rate-of-strain tensor but never with that corresponding to the intermediate eigenvalue. The alignment corresponds closely with the topology; where the topology is stable focus/stretching vorticity is aligned with the largest positive strain and where the topology is unstable focus/contracting it is aligned with the largest negative strain. It is postulated that these kinematic features are not peculiar to the idealised axisymmetric flow studied here but are universal to all processes involving vortex breakdown.

REFERENCES

BROWN, G. L. & LOPEZ, J. M. 1990 Axisymmetric vortex breakdown. Part 2. Physical mechanisms. *J. Fluid Mech.* **221**, 553–576.

CHEN, J. H.; CHONG, M. S.; SORIA, J.; SONDERGAARD, R.; PERRY, A. E.; ROGERS, M.; MOSER, R. & CANTWELL, B. J. 1990 A study of the topology of dissipating motions in direct numerical simulations of time-developing compressible and incompressible mixing layers. *Proceedings of the Center for Turbulence Research Summer Program 1990, Stanford University and NASA Ames Research Center.*

CHONG, M. S.; PERRY A. E. & CANTWELL, B. J. 1990 A general classification of three-dimensional flow fields. *Phys. Fluids A* **2**, 765–777.

ESCUDIER, M. P. 1984 Observations of the flow produced in a cylindrical container by a rotating endwall. *Expts. Fluids* **2**, 189–196.

LOPEZ J. M. 1990 Axisymmetric vortex breakdown. Part 1. Confined swirling flow. *J. Fluid Mech.* **221**, 533–552.

LOPEZ J. M. & PERRY, A. D. 1992 Axisymmetric vortex breakdown. Part 3. Onset of periodic flow and chaotic advection. *J. Fluid Mech.* **234**, 449–471.

PERRY, A. E. & FAIRLIE, B. D. 1974 Critical points in flow patterns. *Adv. Geophys.* **18**, 299–315.

TUCKERMAN, L. S. 1989 Divergence-free velocity fields in nonperiodic geometries. *J. Comp. Phys.* **80**, 403–441.